This article is published as part of the *Dalton Transactions* themed issue entitled:

Dalton Transactions 40th Anniversary

Guest Editor Professor Chris Orvig, Editorial Board Chair
University of British Columbia, Canada

Published in issue 40, 2011 of *Dalton Transactions*

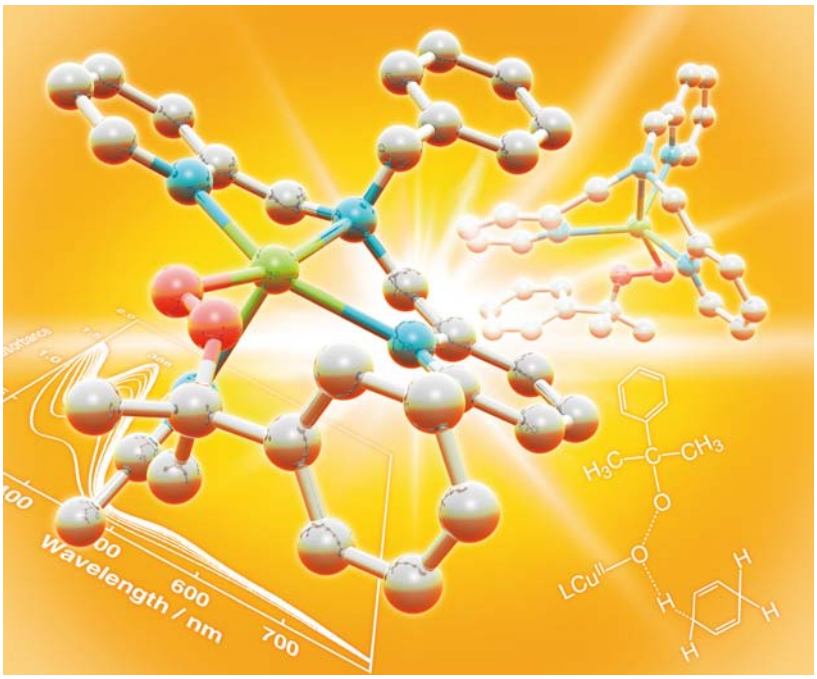

Image reproduced with permission of Shinobu Itoh

Welcome to issue 40 of the 40th volume of Dalton Transactions-40/40! Articles in the issue include:

PERSPECTIVE:

FRONTIER:

ARTICLES:

Visit the *Dalton Transactions* website for more cutting-edge inorganic and organometallic research
www.rsc.org/dalton

Dalton Transactions

Dynamic Article Links

Cite this: *Dalton Trans.*, 2011, **40**, 10686

www.rsc.org/dalton

PAPER

Zn(II) Robson macrocycles as templates for chelating diphosphines†

Sergio Ponsico,[a] Henrik Gulyas,[b] Marta Martínez-Belmonte,[a] Eduardo C. Escudero-Adán,[a] Zoraida Freixa*[c] and Piet W. N. M. van Leeuwen*[a]

Received 13th May 2011, Accepted 22nd July 2011
DOI: 10.1039/c1dt10905g

Chelating diphosphines were constructed using dinuclear Zn(II) complexes of Robson macrocycles (Zn-RMCs) as templates. The assembly process is driven by the interaction between the metal centers (Lewis acids) with anionic and neutral Lewis base-functionalized monophosphines. The stability of the final structure depends on the geometry and the affinity of the functional groups of the ditopic phosphines and on the structure of the RMC. In the free ligand the ditopic phosphines coordinate at opposite faces of the pseudo-planar macrocycle as is shown in the molecular structure of several of the assemblies, according to X-ray diffraction. Pre-organization of the system by coordinating the phosphorus atoms to a transition metal center enforced coordination of the functional groups at the same face of the RMC. For several templated diphosphines *cis*-$PtCl_2$ complexes were identified by NMR. The *in situ* assembled diphosphines showed a chelating effect in the rhodium catalyzed hydroformylation of 1-octene. Combination of Zn-RMC **3** and phosphine **A** gave the highest l/*b* ratio (13) in acetonitrile.

Introduction

Organometallic homogeneous catalytic processes can be optimized by tuning the ligand properties. The bite angle of bidentate ligands exerts a dramatic influence on the outcome of several catalyzed reactions.[1,2] In recent years new strategies have been introduced to generate new and large libraries of bidentate ligands for the fine tuning of the catalytic results. Some of them are based on the construction of bidentate ligands using conventional organic reactions[3] to generate covalent bonds (strong interaction), while others are based on supramolecular (weak) interactions[4] between two monodentate ligands,[5,6] such as hydrogen bonding,[1] ionic interactions,[7] or dynamic metal–ligand interactions. For the latter, several strategies have been applied: (a) the use of an "assembly" metal (without catalytic activity) to hold together two monodentate, ditopic ligands,[8,9] (b) incorporation of an "assembly" metal in the structure of one of the monodentate ligands, which interacts with a complementary ditopic ligand,[10] and (c) the application of an external template, containing two metals in its structure, which interact with two ditopic ligands.[11,12] The work presented here falls under the last approach. Salen-like ligands, containing N_2O_2 pockets capable of hosting two metals, are well known and have been extensively studied in the last decades.[13–16] Jacobsen reported the catalytic application of M–salen compounds in enantioselective epoxidation processes.[17] The modular construction of salen ligands enabled the development of sophisticated structures, such as chiral derivatives, the modification of their properties and the development of new generations of ligands.[18] In the early seventies Robson reported[19] a new family of ligands that give binuclear complexes. Robson macrocycles (RMCs) are Schiff-base macrocyclic structures containing a N_4O_2 bis-anionic core based on two phenolate and four imine functionalities. They can coordinate to two dications (such as Zn(II)) generating a bis-cationic metallamacrocycle. These binuclear compounds have been studied in recent years because of their singular structural properties[13–16] and have been applied as platforms for the formation of ladder polymers[20] and other supramolecular structures (*e.g.* porous coordination materials[21]). Like Jacobsen's ligands, RMCs are modular frameworks and their properties can be modified easily by changing their building blocks. For example, with the use of chiral diamines, chiral macrocycles can be obtained.[22–24] This modular nature together with their pseudo-planar geometry makes them interesting candidates for templating agents to generate libraries of bidentate ligands by interaction between their metal centers and different ditopic monophosphines. A similar approach has been previously reported for salphen derivatives.[12,25]

The interaction of Zn(II) metallated tetradentate macrocycles, such as porphyrins[26,27] or salen-like[28] structures with different

[a]*Institute of Chemical Research of Catalonia (ICIQ), Av. Països Catalans 16, 43007, Tarrgaona, Spain. E-mail: pvanleeuwen@iciq.es; Fax: +34 977 920221; Tel: +34 977 920227*

[b]*Department de Química Física i Inorgànica, Universitat Rovira i Virgili, 43007, Tarragona, Spain*

[c]*Facultad de Química de San Sebastián. Universidad del País Vasco, 20080, San Sebastián, Spain, IKERBASQUE, Basque Fundation for Science, 48011, Bilbao, Spain. E-mail: zoraida_freixa@ehu.es*

† Electronic supplementary information (ESI) available: NMR and MALDI-MS spectra and X-ray crystallographic data for **7C**, **9E′**, **8E′**, and **9D′**. CCDC reference numbers 825586–825589. For ESI and crystallographic data in CIF or other electronic format see DOI: 10.1039/c1dt10905g

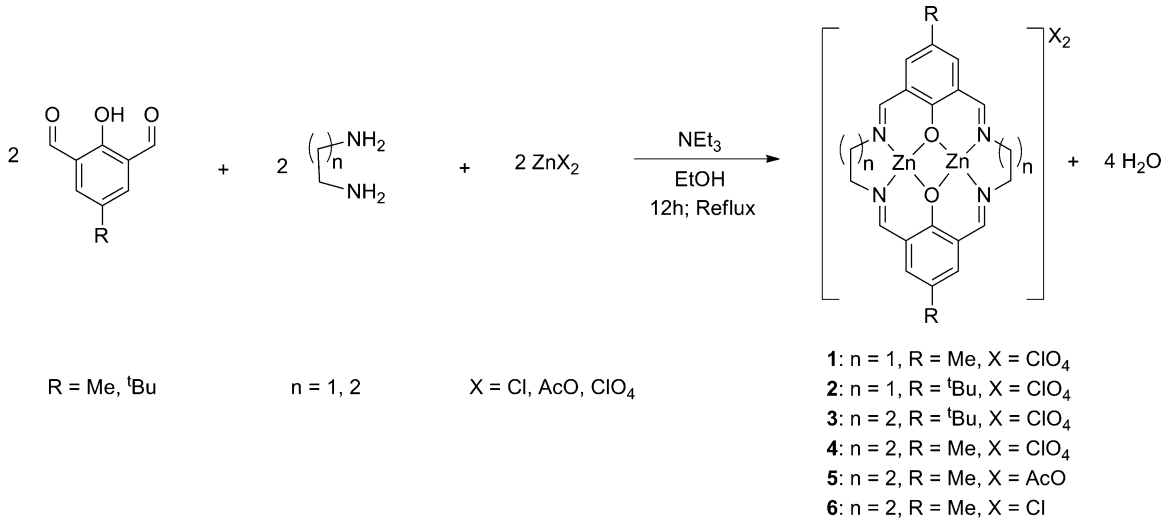

Scheme 1 General synthesis of Zn-Robson macrocycles (Zn-RMCs) **1–6**.

neutral functional groups, is well documented. The coordination of neutral, nitrogen-containing ligands (pyridine, DABCO, quinuclidine) to Zn(II) porphyrins was extensively studied as it became a popular binding motif in supramolecular chemistry.[26,27] The strength of the interaction is well known and association constants were determined for many compounds.[26] The group of Reek van Leeuwen used this binding motif to construct "supramolecular" catalytic entities based on the selective assembly of nitrogen containing phosphines with Zn(II) metallomacrocycles.[29,30] For their use as catalysts at 1 mM concentration the interaction in some instances was just strong enough. We considered that the use of bis-cationic Zn-RMCs as templates would lead to stronger interactions not only with neutral nitrogen donors, but especially with anionic functional groups.[31] These ionic metal–ligand interactions combine the strongest non-covalent interaction (ionic) and the directionality[32] of the dynamic metal–ligand interactions increasing the stability of the final assembled structure. Here we report on the use of metallated RMCs as templates for ditopic ligands, their complexes with Pt, and their use as ligands in Rh catalyzed hydroformylation.

Results and discussion

Robson macrocycle formation

For the synthesis of Zn-RMCs (**1–6**),[33–35] two different isophthalaldehydes were applied in order to introduce different alkyl groups into the macrocyclic structures (Scheme 1). The number of carbon atoms of their substituents influences the solubility of the final ionic compound, the *t*-butyl groups enhancing the solubility in solvents of low polarity. Both isophthalaldehydes were obtained in good yields (76–85%) from a modified Lindoy synthesis.[36]

The synthesis of Zn-RMCs was carried out in the presence of different Zn(II) salts (Scheme 1) in order to study the effect of the counteranion on the macrocycle formation and the self assembly process. Excellent yields (>90%) were obtained when $ZnCl_2$ was used as the metal source. Moderate to good yields (60–80%) were obtained with acetate or perchlorate as the counterion.

The length of the diamine backbone plays a crucial role in the geometry of the final metallamacrocycle. The metallic centers embedded in the RMC can adopt different geometries depending on the N–N linker. For example, when a five-membered ring is formed (n = 1) a square pyramidal geometry around the Zn(II) metal centre is generally observed,[34,37,38] and a few exceptions with octahedral or square planar geometry have been reported for Ni(II)[37] and Cu(I),[39] respectively. Instead, when 1,3-propylenediamine is used (n = 2) a six-membered ring is formed and, although some examples of octahedral geometry of the metal centre can be found,[20,40–42] the formation of a square pyramidal geometry is most common.[20,34,40–48] For larger spacers, forming seven or eight-membered rings, formation of a trigonal bipyramidal geometry around the metal centers can be observed in the solid state.[34,41,49,50] In these structures, the RMC does not retain its planarity. As we were interested in pseudoplanar templates, we decided to study the formation of the RMC using diamines with only two and three carbon atoms as spacers. By changing the N–N linker, not only the geometry around the metal centre can be modified, but also the fluxionality of the final RMC changes.

As observed in the reported molecular structures, metal centers of Zn-RMC (**2**, **3**) are slightly out of the plane of the RMC, in opposite directions, generating a C_2 symmetry axis that passes through the phenolate oxygen atoms. This distortion entails a local differentiation of both sides of the plane of the RMC reflected in the inequivalence of the CH_2 protons (Scheme 2). In the case of **2**, two different groups of signals (4.6 ppm, 3.6 ppm) were observed at room temperature for the CH_2 protons in the ^{1}H-NMR spectrum (supporting information†), belonging to the two faces of the plane. In contrast, for **3** two proton signals were observed for the 1,3-propanediyl spacer, one at 4.07 ppm for the α protons, and the other at 2.20 ppm for the β protons with a 2 : 1 intensity (supporting information†). The equivalence of the protons at both faces in this case indicates rapid interconversion between the conformers of **3** in solution at room temperature. The formation of a six-membered ring facilitates the chair-boat conformational isomerization, which renders these protons equivalent, and also enables a movement of the metals from one side to the other

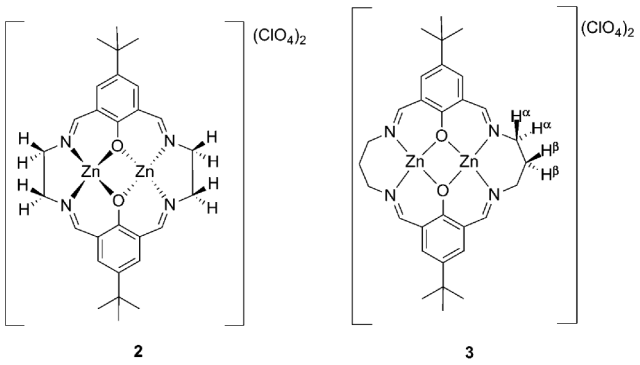

Scheme 2 Diastereotopic protons of **2** and **3**.

of the plane of the macrocycle. These chair and boat conformations could be deduced from the solid state of **9E′** by Single Crystal X-Ray Diffraction (SCXRD) analysis, as will be discussed below.

Construction of the Robson-templated diphosphines

We studied the possibility of using these Zn-RMCs as templates for pyridine, aniline, benzylamine, phenol/phenolate, and benzoic acid/benzoate functionalized phosphines (Scheme 3), for the construction of bidentate ligands. Neutral ligands **A–F** form dicationic assemblies (Scheme 4). It should be noticed that the functional groups of **D**, **E**, and **F** have an acidic proton that can be abstracted with a base in order to generate the anionic **D′**, **E′**, and **F′** ligands that will render the assembled structures neutral (Scheme 5).

Most of the ditopic phosphines, see Scheme 3, were synthesized according to reported methods. 3-Pyridyl phosphine **A**, which is usually synthesized by the reaction of 3-pyridyllithium and chlorodiphenylphosphine,[51] was obtained in high yield by the Steltzer method,[52] *i.e.* Pd-catalyzed P–C coupling of diphenylphosphine and 3-iodopyridine.

The nature of the counterion of the RMC plays a dominant role in the outcome of the formation of the self-assemblies. As

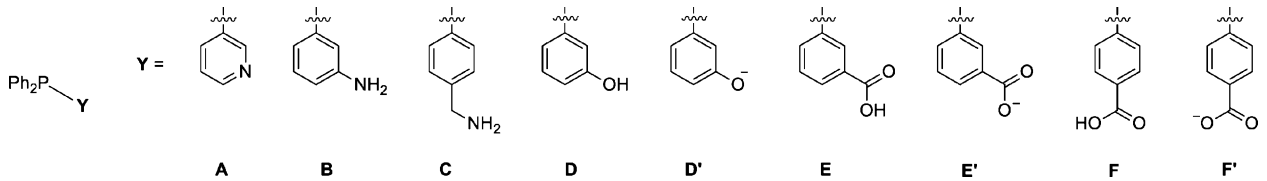

Scheme 3 Functionalized monophosphines employed to build the assemblies.

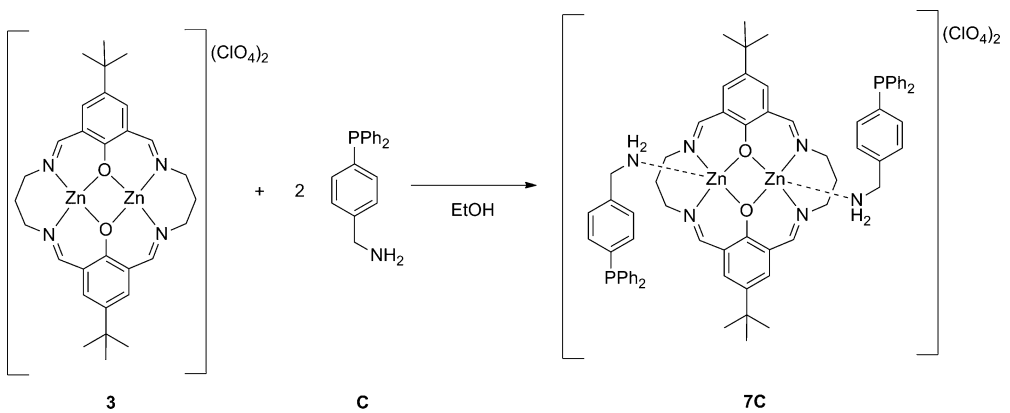

Scheme 4 Ionic self-assembled bidentate ligands.

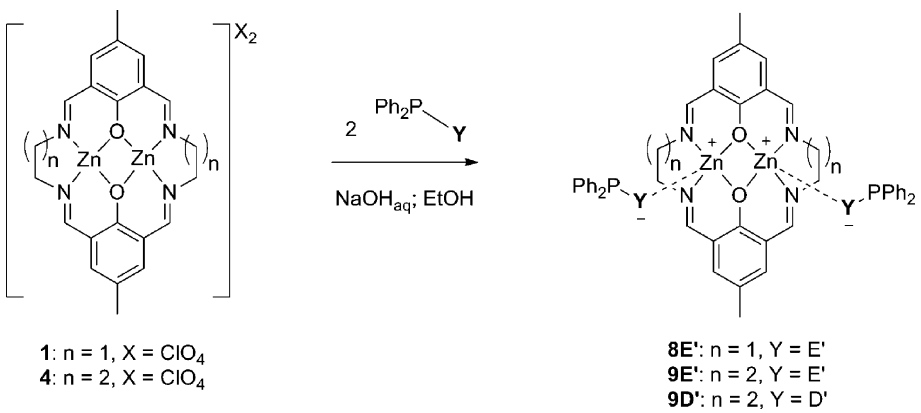

Scheme 5 Neutral self-assembled bidentate ligands.

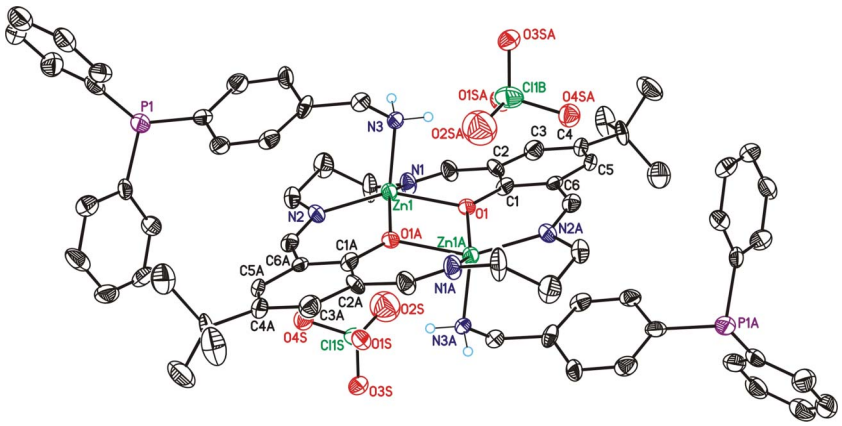

Fig. 1 ORTEP representation of **7C** (some hydrogen atoms and solvent molecules have been omitted for clarity. Thermal ellipsoids are drawn at 50% probability level. "A" denotes symmetry operation: $-x + 1, -y + 1, -z + 1$).

mentioned before, the use of the $ZnCl_2$ as metal precursor for the formation of macrocycles was beneficial, both in terms of yield and purity. However, none of the attempts to substitute the chlorine ion in **6** by any of the monophosphines (**A–F**) was successful, not even when deprotonated **D′–F′** were employed. Instead, the use of the weakly coordinating perchlorate anion permitted the complete formation of the desired assembled products. According to these findings, in spite of the lower yields, Zn(II) salts containing weakly coordinating ions should be used in the synthesis of the RMCs to facilitate their displacement by the ditopic ligand.

To study the formation of the assembly between the RMC and the functionalized phosphines an alcoholic solution of the corresponding phosphine (**A–F**) was added to an alcoholic solution of the RMC. The nitrogen functionalized phosphine **C** produced instantaneously the precipitation of the self-assembled product (Scheme 4) confirming the high affinity of the neutral nitrogen donor towards the cationic Zn(II) metal centers. In the case of the phosphines containing oxygen donor atoms (**D**, **E**, **F**), deprotonation of the functional group with a hard base, such as aqueous NaOH (to generate the corresponding anionic **D′**, **E′**, **F′**), was required to initiate precipitation of the assembled product (Scheme 5). For the weakly coordinating functional groups (**D**, **E**, **F**) no interaction with the cationic Zn(II) metal centre was observed, but upon deprotonation of the protic functional groups the Coulombic contribution strengthens the Lewis acid–base interaction permitting the formation of the assembled diphosphine.

The products obtained were fully characterized by MALDI-TOF-MS and NMR spectroscopy. Molecular structures of compounds **7C**, **8E′**, **9D′** and **9E′** were obtained by X-ray diffraction of crystalline samples. Visual inspection of **7C** and **9E′** (Fig. 1 and Fig. 2) confirms that the RMC templates are nearly planar, and in both structures the two metal centers deviate symmetrically (0.519 and 0.526 Å, respectively) from this plane in opposite directions. The geometry around the Zn(II) metal center corresponds in both cases to a slightly distorted square pyramid (Table 1,2), as expected for this type of RMC. The Zn(II) central atoms are out of the plane of the N_2O_2 pocket, which constitutes the base of the square pyramidal coordination, and the apical position is occupied by the functional groups of the monophosphine. In solution, both compounds (**7C** and **9E′**) are C_{2h} symmetric, as indicated by the high symmetry of the ^{1}H-NMR spectra (see experimental), but in the solid state, due to the fixed orientation of phosphines, the symmetry is reduced to C_i. Additionally, as the assembly is dicationic, the perchlorate counterion is present in the final structure of **7C**; it is located close to the cationic metal centre, but on the opposite side of the N_2O_2 plane with respect to the functional group of **C**. Instead, compound **9E′** (Fig. 2) forms a neutral assembly, as ligand **E′** is anionic. The ionic interaction with the metal center is stronger than the neutral Lewis acid–base M–N interaction; this can be noticed in the shorter distance of the functional group to Zn, the longer distance between Zn and the imine nitrogens, and the larger distance of the metal to the N_2O_2 pocket observed in this structure when compared with the distances in **7C**. The carboxylate group of **E′** enforces a perpendicular disposition of the benzoate aromatic ring, unlike the structure of **7C**, perhaps due to a repulsion between the oxygen atoms (O3,O1) or crystal packing forces. This is reflected in the lack of coplanarity of the RMC. A distance of 0.536 Å can be measured between the two parallel planes containing phenol carbons from C1 to C6 (nearly coplanar in the case of **7C**).

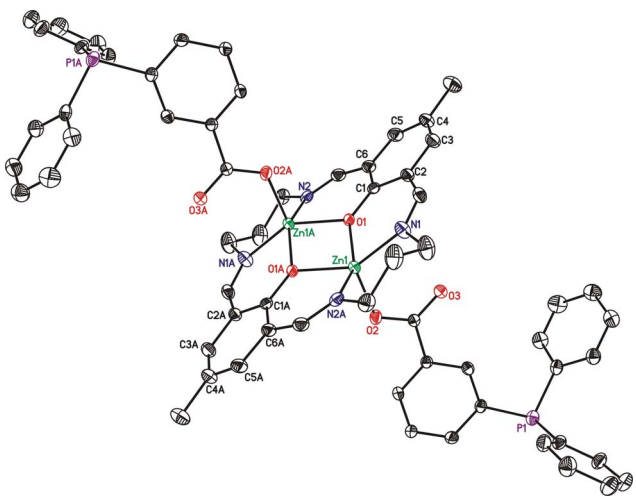

Fig. 2 ORTEP representation of **9E′** (hydrogen atoms and solvent molecules have been omitted for clarity. Thermal ellipsoids are drawn at 50% probability level. "A" denotes symmetry operation: $-x + 1, -y + 1, -z + 2$).

Table 1 Selected bond lengths, angles, and geometrical parameters for **7C**

Zn1–N3	2.077(6)	N1–Zn1–O1A	144.9(2)
Zn1–N1	2.052(7)	N2–Zn1–O1	153.1(2)
Zn1–N2	2.056(6)	N1–Zn1–O1	85.8(2)
Zn1–O1	2.110(5)	O1–Zn1–O1A	75.3(2)
Zn1–O1A	2.008(5)	O1A–Zn1–N2	90.0(2)
		N2–Zn1–N1	94.4(3)
Zn1 ··· O2S	3.643	N3–Zn1–N1	107.1(3)
Zn1 ··· α	0.519	N3–Zn1–N2	114.2(3)
δ ··· δ′	0.003	N3–Zn1–O1	91.3(2)
P1 ··· P1A	16.186	N3–Zn1–O1A	102.6(2)
		β ^ γ	19.36
		N3–Zn1 ··· O2S	169.51

Symmetry code: A $-x + 1, -y + 1, -z + 1$ α: plane formed by N1, N2, O1, O1A; β: plane formed by N1, N1A, N2, N2A; γ: plane formed by Zn1, O1, Zn1A, O1A; δ: plane formed by C from C1 to C6; δ′: plane formed by C from C1A to C7A.

Table 2 Selected bond lengths, angles, and geometrical parameters for **9E′**

Zn1–O2	1.974(2)	N1–Zn1–O1A	145.93(12)
Zn1–N1	2.075(3)	N2A–Zn1–O1	152.81(11)
Zn1–N2A	2.108(3)	N1–Zn1–O1	87.74(10)
Zn1–O1	2.0656(17)	O1–Zn1–O1A	76.92(9)
Zn1–O1A	2.028(2)	O1A–Zn1–N2A	88.12(9)
		N2A–Zn1–N1	92.51(10)
N1 ··· O3	3.138	O2–Zn1–N1	114.73(12)
Zn1 ··· α	0.526	O2–Zn1–N2A	98.18(10)
δ ··· δ′	0.537	O2–Zn1–O1	106.39(10)
P1 ··· P1	18.276	O2–Zn1–O1A	98.83(11)
		β ^ γ	19.87

Symmetry code: A $-x + 1, -y + 1, -z + 2$ α: plane formed by N1, N2, O1, O1A; β: plane formed by N1, N1A, N2, N2A; γ: plane formed by Zn1, O1, Zn1A, O1A; δ: plane formed by C from C1 to C6; δ′: plane formed by C from C1A to C7A.

In both compounds the interaction between the functional groups of the monophosphines and the two metal centers of the Zn-RMC occurs on opposite faces of the pseudoplane of the macrocycle. This is assigned to steric repulsion, as observed previously for other templates.[25] This arrangement is not the most appropriate one for the use of these assemblies as chelating diphosphines, and it may well constitute a drawback.

The analysis by X-ray diffraction of the molecular structure of **9E′** shows some disorder due to the above mentioned chair-boat structural fluxionality (Fig. 3). Although this disorder affects the whole molecule, the most important difference between the two dispositions is the conformation of the six-membered ring of the metallated RMC. In the most abundant configuration, with 78% occupancy, the six-membered ring adopts a chair like conformation; in the other one, having 22% occupancy, the six-membered ring shows a boat like conformation. From this experimental observation it can be concluded that the two chair-boat conformations, postulated before (*vide supra*) for the RMCs containing a 1,3-propanediamine linker, are indeed observed in the solid state at low temperature (100 K). It is expected that as a result of this high flexibility of the RMCs derived from **3**, these will be able to interact with two donor groups at the same face of the macrocycle, enabling that way the formation of chelating bidentate ligands.

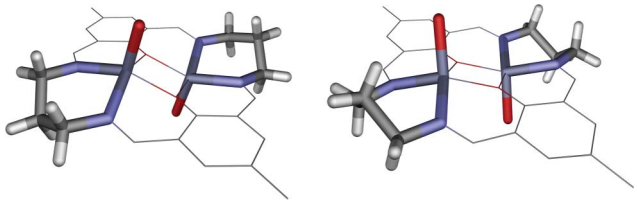

Fig. 3 Fragmented representation (PPh_2Ar, solvent, and some hydrogens omitted for clarity) of the two configurations observed by SCXRD analysis of **9E′**: chair 78% occupancy (left) and boat 22% occupancy (right).

Complexation studies of the assembled diphosphines

Several attempts to coordinate the assembled diphosphines (**7C**, **8E′**, **9D′**, **9E′**) to transition metals, such as Pt(II) and Rh(I), resulted in the formation of insoluble solids, most probably due to the formation of polymeric structures. The key problem when using these bimetallic flat templates is how to direct the orientation of the phosphines, originally located on different faces of the template, toward the same one. Previously reported observations on salen templates[25] indicated that the ditopic ligands moved to the same face of the macrocycle when a transition metal was added, which enabled the formation of the desired bidentate ligand. These bis-salen molecules are less distorted than the ones presented here, their metal–ligand bonds are weaker, and also the zinc atoms are farther apart and can act independently. Apparently this is not the case when preformed Zn-RMC templated diphosphines are used, and the assembled ligands probably remain in their "transoid" non-chelating arrangement even in the presence of a transition metal.

To circumvent this problem, we assayed the construction of the supramolecular complexes by coordinating the two functionalized phosphines to a transition metal centre prior to the addition of the macrocycle. We believe that this pre-organization might facilitate the "*cis*-side" interaction between the functional groups of the monophosphines and the metallic centers of the Zn-RMC (Scheme 6 and Scheme 7).

In order to test this hypothesis, reactions of triarylphosphines (**A**, **B** and **D–F**) with $Pt(COD)Cl_2$ were studied in deuterated dichloromethane by $^{31}P\{^1H\}$-NMR spectroscopy (Table 3), in a 2 : 1 ratio. In all cases, the corresponding *cis* square planar complexes were obtained (**10A**, **10B** and **10D–10F**) as the major products (see experimental). In some cases minor impurities were also formed, *i.e.* a species with three phosphorus atoms coordinating to the Pt metal centre was observed in the case of **D** (26.73 ppm (2P, d, $J_{P\text{-}P}$ = 18 Hz, $J_{Pt\text{-}P}$ = 2489 Hz), 16.16 ppm (1P, t, $J_{P\text{-}P}$ = 18 Hz)). The values of $J_{Pt\text{-}P}$ observed for **10A**, **10B** and **10D–10F**, of approximately 3600 Hz, clearly indicate that the chloride ligands are *trans* to the phosphorus atoms.[7,53] The *cis* coordination mode of the phosphorus atoms in these Pt complexes should pre-organize the system favoring the interaction with the Zn-RMC. Indeed, when one equivalent of the Zn-RMC was added to the complexes **10**, a well-defined change in the $^{31}P\{^1H\}$-NMR spectrum of the major product could be observed (Table 3). Coordination of the functional groups, pyridyl (**A**), amino (**B**) and hydroxyl (**D**), to the Zn atoms of the RMC resulted in a 4–5 ppm upfield shift of the phosphorus signals of the Pt-complexes, and a considerable, 350–400 Hz, decrease in the $J_{Pt\text{-}P}$ coupling constants (Table 3, Entries 1–3 and 8–10, Fig. 4).

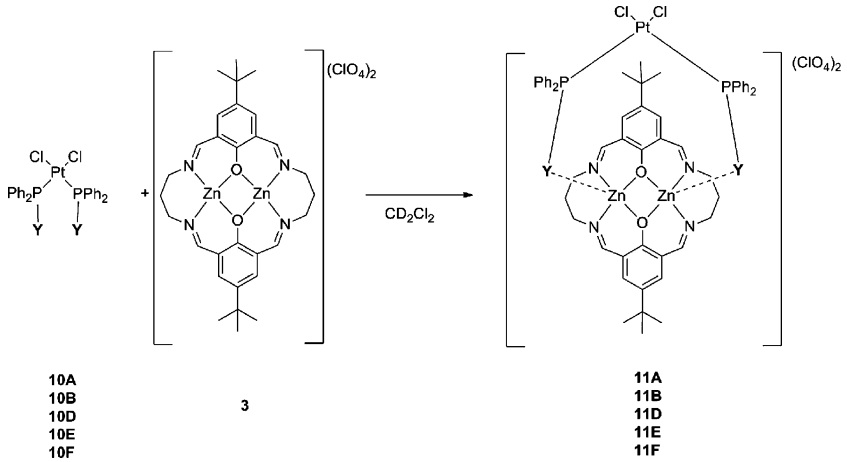

Scheme 6 Neutral Pt templated assemblies.

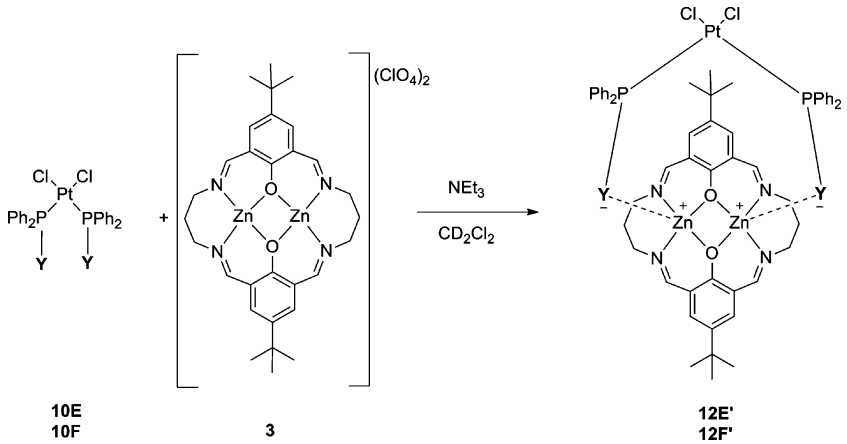

Scheme 7 Ionic Pt templated assemblies.

Table 3 Main products observed by $^{31}P\{^{1}H\}$-NMR in CD_2Cl_2

$Pt(PPh_2Y)_2Cl_2$			
Entry	Compound	δ (ppm)	J_{P-Pt} (Hz)
1	**10A**	13.33	3660
2	**10B**	17.30	3692
3	**10D**	17.01	3696
4	**10E**	17.26	3669
5	**10E′**	16.95	3699
6	**10F**	17.36[a]	3659[a]
7	**10F′**	16.80[a]	3673[a]
		16.80[b]	3685[b]
$Pt(PPh_2Y)_2Cl_2$ + RMC			
Entry	Compound	δ (ppm)	J_{P-Pt} (Hz)
8	**11A**	7.92	3287
9	**11B**	11.79	3310
10	**11D**	11.67	3304
11	**10E** + **3**	17.04	3674
12	**12E′**	12.08	3230
13	**10F** + **3**	17.06[a]	3672[a]
14	**12F′**	11.75[a]	3266[a]
		11.54[b]	3282[b]

[Pt] = 20 mM.[a] Method 1. [b] Method 2.

It should be emphasized that coupling constants around 3300 Hz still correspond to *cis* complexes, but the electronic and steric properties of the assembled diphosphines **11** are evidently different from those of the non-assembled monophosphines **10**. Although the interaction between the donor groups in PPh_2Y and the macrocycle may decrease slightly the electron density on the phosphorus atom, we rather attribute the spectroscopic changes observed to a change in the geometry of the phosphine. The ^{31}P chemical shift and the coupling constants in complexes strongly depend on the geometry, as reported.[54,55] Although this effect could be clearly observed, other products were also present in the $^{31}P\{^{1}H\}$-NMR spectra (supporting information†); for example in the case of **D** a new signal appears at 23.29 ppm with a J_{Pt-P}coupling of 3094 Hz that could correspond to other geometries around the Pt(II) metal centre.

Interesting phenomena were observed when platinum complexes of the carboxylated monophosphines (**E**, **F**) were combined with the Zn-RMC. When one equivalent of **3** was added to platinum complex **10E** in order to form **11E**, unlike in previous examples, only minor changes were observed in the $^{31}P\{^{1}H\}$-NMR, that is a slight upfield shift in the main signal (Table 3, Entry 11) and the appearance of a tiny signal at 11.24 ppm (supporting information†). When two equivalents of triethylamine were added to this mixture, new products appeared in the $^{31}P\{^{1}H\}$-NMR

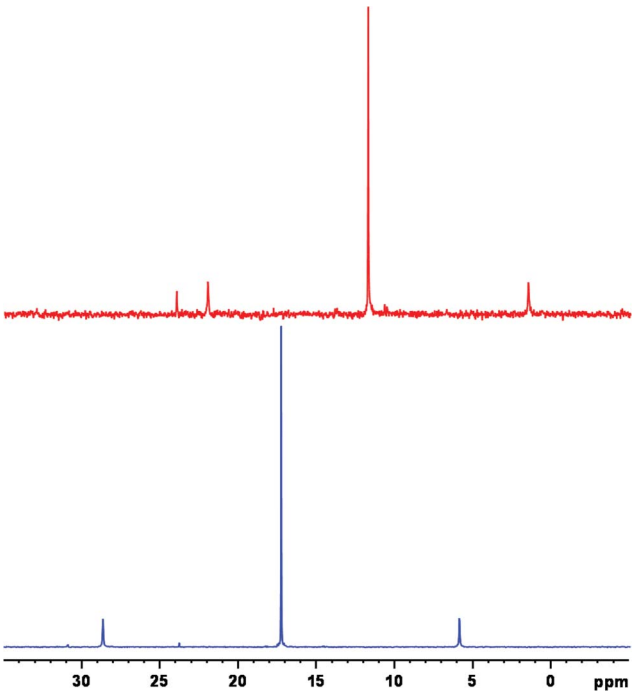

Fig. 4 $^{31}P\{^{1}H\}$-NMR of **10B** (blue, bottom) and **11B** (red, top).

spectrum. The chemical shift of the major signal is 5 ppm upfield and the J_{Pt-P} coupling constant about 440 Hz smaller than that of the original platinum complex of the monophosphine (Table 3, Entry 12). This NMR pattern is very similar to those observed for **A**, **B**, and **D** derivatives, and thus we conclude that the addition of base initiates the formation of the fully assembled structure **12E′** (Scheme 7), suggesting that, upon deprotonation, the carboxylate groups have stronger affinity for the RMC. In the same NMR spectrum other signals could be observed; on the one hand, a signal similar to the original platinum complex **10E**, but with slightly different chemical shift and J_{Pt-P} coupling constant that could correspond to the Pt(II) complex with the deprotonated ligand **10E′**, and on the other hand a set of 2 doublets (see experimental) that corresponds to a desymmetrization of the two phosphorus atoms around the transition metal centre, but still coordinated to it as indicated by the chemical shift and the coupling constants (see experimental). The existence of these compounds indicates that even after deprotonation most of the carboxylates remain uncoordinated to the Zn-RMC.

A similar behavior was observed for ligand **F** when the same procedure (Method 1) was applied. When one equivalent of **3** was added to platinum complex **10F** in order to form **11F**, no major change in the $^{31}P\{^{1}H\}$-NMR was observed (Table 3, Entry 13, Fig. 5), but when two equivalents of triethylamine were added to this mixture, new products appeared in the $^{31}P\{^{1}H\}$-NMR spectrum: a major signal (**12F′**) 4 ppm upfield and J_{Pt-P} coupling constant about 400 Hz smaller than that of **10F**, a signal (**10F′**) similar to **10F**, and a set of 2 doublets (see experimental).

Using the same procedure (Method 1) platinum complex **10E′**, containing the *meta*-carboxylated monophosphine (**E′**), forms the fully assembled product **12E′** to a lower extent (40% by NMR integration) and the signal is broader than that of **12F′** having *para*-substituted monophosphines (58% by NMR integration). This finding demonstrates that the stability of the assembled

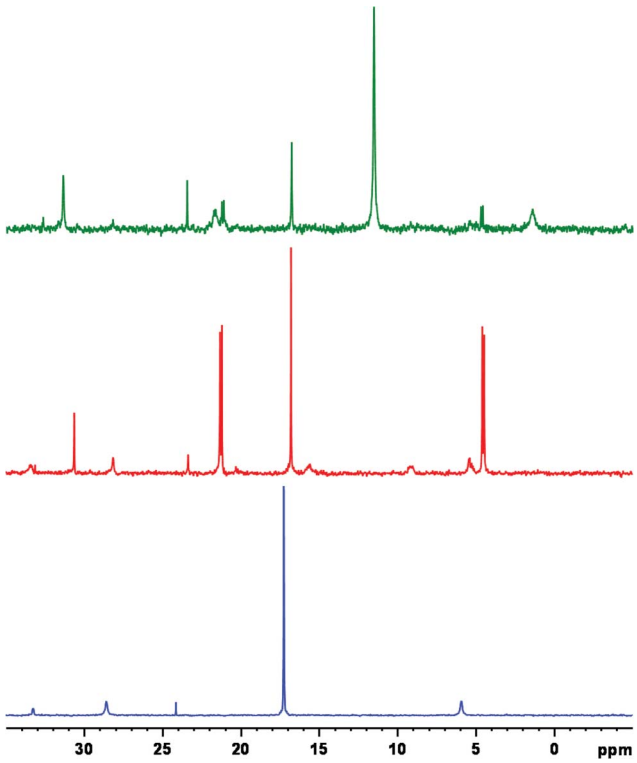

Fig. 5 $^{31}P\{^{1}H\}$-NMR of **10F** (blue, bottom), **10F** + base (red, middle), and **12F′** (**10F** + base + **3**) (green, top).

product also depends on the geometry of the ditopic ligand. In the MALDI-TOF-MS analysis (Fig. 6) of the reaction mixture the molecular mass of the assembled complex **12E′** was detected showing the appropriate isotopic distribution pattern compared to the calculated one, providing additional evidence for the formation of the desired product.

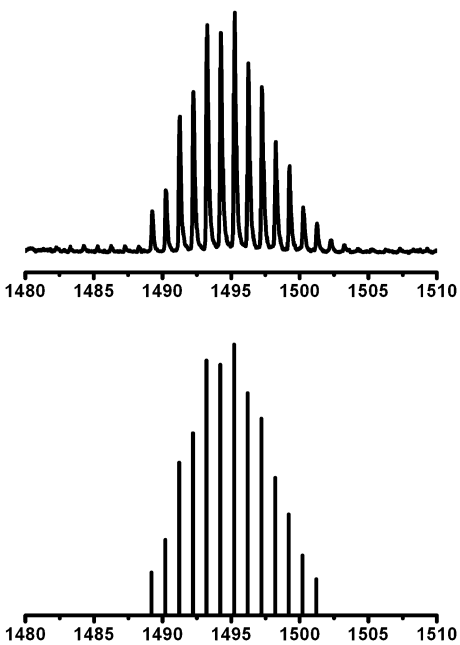

Fig. 6 Isotopic distribution pattern of **12E′**: experimental by MALDI-TOF-MS (top), and calculated (bottom).

Table 4 Rhodium catalyzed hydroformylation of 1-octene

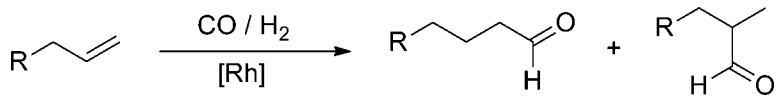

Entry	Ligand	RMC	Solvent	T/°C	Time (h)	Conversion (%)	Isomerization (%)	TOF[a,c]	l/b[b]
1	Me–xantphos	—	Toluene	60	5.13	15.4	1.6	20 (15)	48.9
2	PPh_3	—	Toluene	60	3.16	97.5	1.8	345 (42)	2.9
3	—	—	Toluene	60	2.34	98.3	56.5	332 (59)	2.6
4	—	**5**	Toluene	60	5.21	8.7	4.6	11 (9)	2.8
5	**A**	—	Toluene	60	4.08	97.6	1.5	348 (27)	2.9
6	**A**	—	THF	50	4.88	55.8	0.7	86 (27)	2.8
7	**A**	—	Acetonitrile	60	7.84	94.8	1.5	160 (35)	2.9
8	**A**	**3**	Toluene	60	4.68	96.7	1.5	271 (25)	2.9
9	**A**	**3**	THF	50	4.92	23.9	0	33 (24)	2.8
10	**A**	**3**	Ethyl acetate	60	2.6	22.4	0	58 (22)	2.9
11	**A**	**3**	2-Butanone	60	7.23	50.1	4.0	65 (24)	7.4
12	**A**	**3**	Dichloroethane	60	4.98	48.2	4.1	72 (20)	9.7
13	**A**	**3**	Acetonitrile	60	5.16	39.2	5.7	67 (22)	13.0
14	**A**	**2**	Acetonitrile	60	7.18	35.8	1.4	36 (22)	4.1
15	**B**	**3**	Acetonitrile	60	8.00	60.0	0	73 (20)	2.4
16	**C**	**3**	Acetonitrile	60	4.44	95.3	1.2	253 (20)	2.5
17	**C**	**3**	Dichloroethane	60	3.27	98.8	1.3	298 (30)	2.5
18	**D**	**3**	Acetonitrile	60	2.44	48.3	2.6	132 (20)	2.2
19	**D**	**3**	Dichloroethane	60	8.75	97.9	0.4	89 (47)	2.6
20	**E**	**3**	Acetonitrile	60	8.04	88.2	0.4	155 (22)	2.8
21	**F**	**3**	Acetonitrile	60	7.8	<1	0.3	<1	1.7
22	**F**	**3**	Dichloroethane	60	5.71	82.7	0	78 (26)	2.7

Incubation: $CO:H_2$ (1 : 1); 20 bar; 80 °C; 90 min. Reaction: $CO:H_2$ (1 : 1); 20 bar; P : Rh (10 : 1); 1-octene : Rh (670 : 1); RMC : ligand (1 : 2); [Rh] = 1 mM.[a] Turnover frequency in (mol aldehyde) (mol Rh)$^{-1}$ h^{-1}. [b] Linear to branched aldehyde ratio. [c] In parentheses the conversion at which the TOF was calculated.

We decided to invert the addition order for the formation of **12F′**, adding first the base and then the RMC (Method 2) to **10F**. When two equivalents of triethylamine were added to **10F**, in the absence of any RMC, **10F′** appeared in the $^{31}P\{^1H\}$-NMR spectrum as a slightly upfield shift and the J_{Pt-P} coupling constant slightly decreased (Table 3, Entry 7) and the set of 2 doublets (21.19 ppm, J_{P-Pt} = 3945 Hz; 4.66 ppm, J_{P-Pt} = 3589; Hz J_{P-P} = 18 Hz) similar to the one described for phosphine **E′** was also observed (Fig. 5). Although we are not certain about the nature of the species responsible of these two signals, it could well be that a deprotonated carboxylate coordinates to the Pt(II) metal center differentiating the two phosphorus atoms; these species may be cyclic oligomers. After addition of RMC **3** to that mixture the main signal corresponds to a species containing equivalent phosphorus nuclei (Fig. 5). The singlet character, the chemical shift, and the J_{Pt-P} coupling constant of this signal correspond to the fully assembled product **12F′** (Table 3, Entry 14) previously observed. It should be noted that using this Method 2 the $^{31}P\{^1H\}$-NMR spectrum is much cleaner than the one obtained by Method 1, as eventually the set of doublets almost disappears. This observation indicates that the addition order of the base and the RMC to **10F** has an important influence in the formation of the fully assembled complex **12F**.

Catalytic application of the assembled diphosphines

Monophosphines and chelating diphosphines show different performance as ligands in rhodium catalyzed hydroformylation of 1-alkenes.[2,56] One of the effects of chelating bidentate ligands is a decrease in activity compared to the activity of the rhodium complexes of structurally similar monodentate ligands. This difference between the activities can be rationalized by the fact that monodentate ligands are more prone to dissociation than the bidentate ones facilitating the coordination of the reactants to the rhodium central atom. Another characteristic effect of diphosphines, if they have the appropriate bite angle, is that they can dramatically increase the regioselectivity of the hydroformylation reaction. It has been observed that ligands with natural bite angles[56–58] around 110° prefer a diequatorial coordination mode to equatorial–apical chelation in the catalytically active trigonal bipyramidal (bidentate P-ligand)$Rh(CO)_2H$ complexes, which ultimately leads to a higher linear : branched ratio.

The assembled ligands presented here were tested in the Rh-catalyzed hydroformylation of 1-octene in order to probe the robustness of the assemblies and their coordinating properties under catalytic conditions.

The assembled bidentate ligands were formed *in situ* by mixing a solution containing the ditopic phosphine and the corresponding Rh(I) precursor with the solution/suspension of the Zn-RMC, in the autoclave. The P : Rh : Zn-RMC ratio was 2 : 1 : 1 in all cases.

The hydroformylation reactions were carried out at 50–60 °C, 20 bar of synthesis gas ($CO:H_2$ 1 : 1), and in a range of non-protic solvents (Table 4). As reference for monodentate and bidentate ligands triphenylphosphine and Me–xantphos were tested under the same reaction conditions (Entries 1 and 2). As is well known, in the absence of ligand the substrate is rapidly consumed but the main products are the isomerization products (Entry 3).

When one of the Zn-RMC (**5**) was tested under the same conditions in absence of phosphine ligand (Entry 4) the activity is dramatically reduced; this lack of activity could be due to Zn/Rh

transmetalation or formation of aggregates thus trapping rhodium in an inactive form, as isomerization was not observed either.

For comparison, the ditopic ligand **A** was first tested under the same reaction conditions in the absence of the templating agent Zn-RMC (Entries 5–7). As expected, the ditopic ligand alone behaves as PPh_3 (Entries 2 and 5), showing high activities but low linearity in the product. Although there is some influence of the solvent on the activity (TOF) no major changes in the selectivity (l/*b* ratio) were observed.

The addition of Zn-RMC **3** led to slower catalytic systems (Entries 5 and 8, 6 and 9, 7 and 13), most likely due to a bidentate effect resulting from the formation of the supramolecular chelate. From the NMR studies on platinum chloride it was known that formation of phosphine complexes prior to the addition of the RMC favoured the formation of bidentate ligand systems, but in view of the incubation at high temperature and the reaction temperature this was not necessary for the catalytic studies.

Only in acetonitrile the drop in activity is accompanied by a spectacular improvement of the selectivity (from 2.9 to 13.0) whilst in other solvents it remains basically unaltered after addition of template **3**. For toluene, THF, and ethyl acetate as the solvent (Entries 8–10) low selectivities were obtained, but when 2-butanone, dichloroethane, and acetonitrile (Entries 11–13) were used, the selectivity to the linear aldehyde went up to a l/*b* ratio of 13. The solvent may influence the rate of formation of the bidentate assembly ligands and/or the equilibrium. As mentioned above, this may be a disadvantage of the supramolecular approach, in that the formation of the desired species is not always sufficiently fast. Acetonitrile may facilitate rearrangements of the complexes to the desired bidentate ligands, but for dichloroethane this is not obvious.

The best two solvents for **A**, dichloroethane and acetonitrile, were used to test ditopic ligands **B–F**, but much lower selectivities were obtained than those encountered for ligand **A**. The low l/*b* ratios and relatively high activities found for **C**, **D**, and **E** are typical of monophosphines (entries 2 and 7), which indicates that these ligands do not give the desired assembly to a large extent. Ditopic ligands **B** and **C** containing *N*-donors did form the corresponding Pt-assemblies as was observed by NMR spectroscopy, albeit at higher concentrations, and perhaps the rhodium ligated species are not formed for steric reasons or because of the stoichiometry used. The weak O–Zn interaction, already observed at the concentrations used in the NMR experiments, may account for the weakness of the assembly in the case of ligands **D–F**. Furthermore, the carboxylic acid function of **F** may hamper the formation of rhodium hydride, as excess of carboxylic acids will do so.[59]

When templating agent **3** in complexes of ligand **A** was changed for the more rigid one **2** (Entry 14), the selectivity is lower than that obtained for **3**, but it is still higher than that of the free ligand.

Conclusions

Zn-RMCs were applied as templating agents to generate self-assembled bidentate ligands. Zn(II) metal centres of RMCs interact with both neutral and anionic Lewis base functionalized monophosphines to give supramolecular diphosphines. When two ditopic ligands coordinate to the Zn-RMC they do so at opposite faces minimizing steric repulsion. The assembly formed this way cannot act as a chelating diphosphine. From the two types of templates studied, Zn-RMCs containing propylenediamine linkers constitute much more flexible platforms than the ones containing ethylenediamine spacers. When the former platforms are used, addition of a transition metal forces the functional groups of the phosphine to coordinate to the Zn-RMC on the same face. The *in situ* assembled diphosphines showed a chelating effect in the rhodium catalyzed hydroformylation of 1-octene probing the presence of a supramolecular interaction under catalytic conditions and the robustness of the system. In a few systems containing the propylenedianine RMC an increased preference for linear aldehyde formation was found (l/*b* = 13 : 1), indicative of a wide bite angle. The ethylenediamine RMC with the same pyridylphosphine ditopic ligand gave only a modest increase in the l/*b* ratio. The nature of the solvent plays a crucial role, which is not understood. The results evidence that many factors influence the stability of the supramolecular assembly; structure and electronic nature of the ditopic ligand, rigidity of the template and solvent must be carefully selected to guarantee the robustness of the system under catalytic conditions. The intermediate strength of the pyridyl group to Zn gave the best results in catalysis. The desired stronger bonding of the anionic groups retard the formation of the assemblies that can function as bidentates and they give inactive rhodium complexes. Thus, although a wide variety of new bidentate phosphines can be readily obtained, their applicability in catalysis is limited.

Experimental

General

Warning: solid perchlorate complexes containing organic ligands are potentially dangerous and should be handled with care.

5-*tert*-Butylphenol, *para*-cresol, hexamethylenetetramine, 1,3-diaminopropane, 1,2-diaminoethane, 1,2-diaminobenzene, zinc(II) perchlorate hexahydrate, zinc(II) tetrafloroborate hydrate, zinc(II) acetate dihydrate, zinc(II) chloride, 3-iodopyridine, and deuterated solvents were purchased from Sigma-Aldrich and used as received. Triethylamine, trifluoroacetic acid 99%, palladium(II) acetate trimer were purchased from Alfa–Aesar and used as received. Dichloro(1,5-cyclo-octadiene)platinum(II) was purchased from Across and used as received. RMC,[33,35,60] *meta*-(diphenylphosphino)benzoic acid,[52] *para*-(diphenylphosphino)benzoic acid,[52] (3-(diphenyl-phosphino)phenyl)methanamine,[61] 3-(diphenylphosphino)-aniline,[7] 3-(diphenylphosphino)phenol,[59] diphenylphosphine,[7] and 4,5-(dihexyloxy)-1,2-diaminobenzene[62] were synthesized according to the literature. All manipulation of phosphorous containing products was carried out under Argon atmosphere using Schlenk techniques. Methanol and ethanol absolute reagent grade for RMC synthesis were purchased from Scharlau and used as received. Solvents were purchased from Sigma–Aldrich as HPLC grade, dried with an SPS system of ITC-inc. and degassed using standard methods. NMR spectra unless otherwise stated were recorded using a Bruker ATM-400 spectrometer operating at the following frequencies: 400.13 MHz (^{1}H), 161.98 MHz (^{31}P). ^{31}P NMR spectra were recorded using broad band decoupling. Chemical shifts of ^{1}H NMR spectra are reported in ppm downfield from TMS, used as internal standard. Chemical shifts of ^{31}P NMR spectra are referred to H_3PO_4 as an external standard.

Synthesis of ditopic ligands

3-(Diphenylphosphino)pyridine (A). Synthesized according to a modified Steltzer[52] procedure: 3-iodopyridine (1 g, 4.9 mmol) and palladium acetate (2 mg, 0.0034 mmol) were dissolved in acetonitrile (20 mL) under inert atmosphere. Triethylamine (4.9 mmol) and diphenylphosphine (0.912 g, 4.9 mmol) were added to the reaction mixture, and it was stirred at 85 °C for 24 h. The full conversion was confirmed by $^{31}P\{^{1}H\}$-NMR. The solvent was removed *in vacuo*. The residue was dissolved in dichloromethane (20 mL), and the organic solution was washed with water (3 × 20 mL). The aqueous extract was washed with Et_2O (20 mL), and the combined organic phase was dried over $MgSO_4$. After filtration and solvent removal, the residue was purified by flash chromatography (silica, EtOAc). The colorless oily product was recrystallized from hot hexane (10–15 mL). To complete the crystallization the Schlenk tube was left in the freezer (–20 °C) for 2 days. The product was filtered in air obtaining 1.01 g (79% yield) and it was characterized as the reported product.[63]

Synthesis of self assembled diphosphines

7C. A solution of 71.3 mg (0.245 mmol) of diphenylphosphino(*p*-benzylamine) in 10 mL of ethanol was added dropwise over a solution containing 100 mg (0.122 mmol) of **3** in 20 mL of ethanol. The reaction mixture was stirred for 2 h and the white precipitate formed was filtered off and dried in air. 114 mg (66% yield) of a white powder was obtained. A crystalline sample was obtained by slow evaporation of methanol at room temperature and characterized by Single Crystal X-Ray Diffraction (SCXRD). ^{1}H-NMR (400 MHz, $CDCl_3$): 8.17 ppm (s, 4H, imine), 7.36–7.31 ppm (m, 16H), 7.30–7.26 ppm (m, 8H), 7.13 ppm (pseudo t, 7.6 Hz, 4H), 7.02 ppm (d, 7.6 Hz, 4H), 3.88 ppm (br s, 8H), 3.70 ppm (s, 4H), 2.04 ppm (br s, 4H), 1.29 ppm (s, 18H). $^{31}P\{^{1}H\}$-NMR (161 MHz, $CDCl_3$): –3.01 ppm (s).

8E′. A solution of 171 mg (0.560 mmol) of *meta*-(diphenylphosphino)benzoic acid in 10 mL of methanol and 560 µl of $NaOH_{aq}$ 1 M was added dropwise over a solution containing 200 mg (0.280 mmol) of **1** in 10 mL of methanol. The reaction mixture was stirred for 2 h and the white precipitate formed was filtered off from the cold solution and dried in air. 184 mg (59% yield) of a white powder was obtained. A crystalline sample was obtained by slow evaporation of methanol at room temperature in air. SCXRD showed these crystals to be the oxide of the desired product (supporting information†). ^{1}H-NMR (400 MHz, $CDCl_3$): 8.26 ppm (s, 4H, imine), 7.96 ppm (d, 2H, J_{H-P} = 8.8 Hz, H^{Ar}(*ortho*-PPh_2)), 7.81 ppm (d, 2H, J_{H-H} = 6.6 Hz, H^{Ar}(*para*-PPh_2)), 7.30–7.19 ppm (br m), 7.18–7.07 ppm (m, 4H), 7.06 ppm (s, 4H), 4.59–3.62 ppm (br d, 8H), 2.21 ppm (s, 6H). $^{31}P\{^{1}H\}$-NMR (161 MHz, $CDCl_3$): –2.46 ppm (s).

9D′. A solution of 150 mg (0.540 mmol) of 3-(diphenylphosphino)phenol in 5 mL of methanol and 540 µl of $NaOH_{aq}$ 1 M was added dropwise over a solution containing 200 mg (0.270 mmol) of **4** in 5 mL of methanol. The reaction mixture was stirred for 2 h and the white precipitate formed was filtered off from the cold solution and dried in air. 100 mg (quantitative yield) of a white powder was obtained. A crystalline sample was obtained by slow evaporation of methanol at room temperature in air. SCXRD showed these crystals to be the oxide of the desired product (supporting information†). Not characterized by NMR due to its low solubility. MALDI-TOF-MS: 1085.3 ($M + H^+$), 1101.3 ($M + O + H^+$), 1117.3 ($M+2O+H^+$).

9E′. A solution of 50 mg (0.163 mmol) of *meta*-(diphenylphosphino)benzoic acid in 5 mL of methanol and 163 µl of $NaOH_{aq}$ 1 M was added dropwise over a solution containing 61 mg (0.092 mmol) of **4** in 5 mL of methanol. The reaction mixture was stirred for 2 h and the white precipitate formed was filtered off from the cold solution and dried in air. 58 mg (62% yield) of a white powder was obtained. A crystalline sample was obtained by slow evaporation of methanol at room temperature and characterized by SCXRD. ^{1}H-NMR (400 MHz, $CDCl_3$): 8.09 ppm (s, 4H, imine), 7.94 ppm (d, 2H, J_{H-P} = 9.8 Hz, H^{Ar}(*ortho*-PPh_2)), 7.77 ppm (d, 2H, J_{H-H} = 7.6 Hz, H^{Ar}(*para*-PPh_2)), 7.26–7.18 ppm (br m), 7.14–7.05 ppm (m, 4H), 7.04 ppm (s, 4H), 4.06 ppm (m, 8H), 2.20, 2.17 ppm (s, 10H). $^{31}P\{^{1}H\}$-NMR (161 MHz, $CDCl_3$): –2.37 ppm (s). MALDI-TOF-MS: 835.1 (M^+), 851.1 ($M^+ + O$).

Characterization of metal templated assembled diphosphines and intermediate Pt-diphosphine complexes 10

10A and 11A. 3-(Diphenylphosphino)pyridine (7.03 mg, 0.027 mmol) and dichloro(1,5-cyclooctadiene)platinum(II) (5 mg, 0.0134 mmol) were dissolved in 1 mL of deuterated dichloromethane under inert atmosphere. After stirring for 30 min at room temperature the mixture was analyzed by $^{31}P\{^{1}H\}$-NMR (161 MHz, CD_2Cl_2): 28.15 ppm (s), 19.38 ppm (s), 13.33 ppm (s, J_{Pt-P} = 3660 Hz, **10A**). **3** (11 mg, 0.0134 mmol) was dissolved in the same solution. After stirring for 30 min at room temperature the mixture was analyzed by $^{31}P\{^{1}H\}$-NMR (161 MHz, CD_2Cl_2): 29.53 ppm (s), 13.56 ppm (s, J_{Pt-P} = 3644 Hz, **10A**), 7.92 ppm (s, J_{Pt-P} = 3287 Hz, **11A**).

10B and 11B. 3-(Diphenylphosphino)aniline (7.4 mg, 0.027 mmol) and dichloro(1,5-cyclooctadiene)platinum(II) (5 mg, 0.0134 mmol) were dissolved in 1 mL of deuterated dichloromethane under inert atmosphere. After stirring for 30 min at room temperature the mixture was analyzed by $^{31}P\{^{1}H\}$-NMR (161 MHz, CD_2Cl_2): 17.30 ppm (s, J_{Pt-P} = 3692 Hz, **10B**). **3** (11 mg, 0.0134 mmol) was dissolved in the same solution. After stirring for 30 min at room temperature the mixture was analyzed by $^{31}P\{^{1}H\}$-NMR (161 MHz, CD_2Cl_2): 24.00 ppm (s), 11.710 ppm (s, J_{Pt-P} = 3310 Hz, **11B**).

10D and 11D. 3-(Diphenylphosphino)phenol (7.4 mg, 0.027 mmol) and dichloro(1,5-cyclooctadiene)platinum(II) (5 mg, 0.0134 mmol) were dissolved in 1 mL of deuterated dichloromethane under inert atmosphere. After stirring for 30 min at room temperature the mixture was analyzed by $^{31}P\{^{1}H\}$-NMR (161 MHz, CD_2Cl_2): 26.73 ppm (d, J_{P-P} = 18 Hz, J_{Pt-P} = 2489 Hz), 17.01 ppm (s, J_{Pt-P} = 3696 Hz, **10D**), 16.16 ppm (t, J_{P-P} = 18 Hz). **3** (11 mg, 0.0134 mmol) was dissolved in the same solution. After stirring for 30 min at room temperature the mixture was analyzed by $^{31}P\{^{1}H\}$-NMR (161 MHz, CD_2Cl_2): 23.19 ppm (s, J_{Pt-P} = 3094 Hz), 17.12 ppm (s, J_{Pt-P} = 3701 Hz), 11.67 ppm (s, J_{Pt-P} = 3304 Hz, **11D**), and other minor impurities. Solvent was then removed *in vacuo* and the residue analyzed by MALDI-TOF-MS: 1494.2 ($(M - 2(ClO_4) + Cl + H_2O)^+$), 1458.2 ($(M - 2(ClO_4) + OH)^+$), 787.2 ($(Pt + Cl - 2(PR_3))^+$).

10E and 12E′. 3-(Diphenylphosphino)benzoic acid (8.3 mg, 0.027 mmol) and dichloro(1,5-cyclooctadiene)platinum(II) (5 mg, 0.0134 mmol) were dissolved in 1 mL of deuterated dichloromethane under inert atmosphere. After stirring for 30 min at room temperature the mixture was analyzed by $^{31}P\{^{1}H\}$-NMR (161 MHz, CD_2Cl_2): 17.26 ppm (s, J_{Pt-P} = 3669 Hz, **10E**). **3** (11 mg, 0.0134 mmol) was dissolved in the same solution. After stirring for 30 min at room temperature the mixture was analyzed by $^{31}P\{^{1}H\}$-NMR (161 MHz, CD_2Cl_2): 17.04 ppm (s, J_{Pt-P} = 3674 Hz, **10E + 3**), 11.24 ppm (s). Triethylamine (3.8 µl, 0.027 mmol) was added to the solution. After stirring for 30 min at room temperature the mixture was analyzed by $^{31}P\{^{1}H\}$-NMR (161 MHz, CD_2Cl_2): 31.47 ppm (s), 18.46 ppm (d, J_{P-P} = 18 Hz), 16.95 ppm (s, J_{Pt-P} = 3699 Hz, **10E′**), 12.08 ppm (s, J_{Pt-P} = 3230 Hz, **12E′**), 4.88 ppm (d, J_{P-P} = 18 Hz, J_{Pt-P} = 3607 Hz). Solvent was then removed *in vacuo* and the residue analyzed by MALDI-TOF-MS: 1489.3 (M^+), 919.4((M – Pt – 2Cl – PR_3)$^+$).

10F, 10F′, and 12F′. **Method 1**: 4-(diphenylphosphino)benzoic acid (8.3 mg, 0.027 mmol) and dichloro(1,5-cyclooctadiene)platinum(II) (5 mg, 0.0134 mmol) were dissolved in 1 mL of deuterated dichloromethane under inert atmosphere. After stirring for 30 min at room temperature the mixture was analyzed by $^{31}P\{^{1}H\}$-NMR (161 MHz, CD_2Cl_2): 17.36 ppm (s, J_{Pt-P} = 3659 Hz, **10F**). **3** (11 mg, 0.0134 mmol) was dissolved in the same solution. After stirring for 30 min at room temperature the mixture was analyzed by $^{31}P\{^{1}H\}$-NMR (161 MHz, CD_2Cl_2): 17.06 ppm (s, J_{Pt-P} = 3672 Hz, **10F + 3**). Triethylamine (3.8 µl, 0.027 mmol) was added to the solution. After stirring for 30 min at room temperature the mixture was analyzed by $^{31}P\{^{1}H\}$-NMR (161 MHz, CD_2Cl_2): 31.22 ppm (s), 23.44 ppm (s), 21.21 ppm (d, J_{P-P} = 20 Hz, J_{Pt-P} = 3918 Hz), 16.80 ppm (s, J_{Pt-P} = 3673 Hz, **10F′**), 11.75 ppm (s, J_{Pt-P} = 3266 Hz, **12F′**), 4.61 ppm (d, J_{P-P} = 20 Hz, J_{Pt-P} = 3592 Hz). **Method 2**: 4-(diphenylphosphino)benzoic acid (8.3 mg, 0.027 mmol) and dichloro(1,5-cyclooctadiene)platinum(II) (5 mg, 0.0134 mmol) were dissolved in 1 mL of deuterated dichloromethane under inert atmosphere, and stirred for 30 min at room temperature. Triethylamine (3.8 µl, 0.027 mmol) was added to the solution. After stirring for 30 min at room temperature the mixture was analyzed by $^{31}P\{^{1}H\}$-NMR (161 MHz, CD_2Cl_2): 30.63 ppm (s), 21.26 ppm (d, J_{P-P} = 20 Hz, J_{Pt-P} = 3945 Hz), 16.80 ppm (s, J_{Pt-P} = 3685 Hz, **10F′**), 4.54 ppm (d, J_{P-P} = 20 Hz, J_{Pt-P} = 3589 Hz). **3** (11 mg, 0.0134 mmol) was dissolved in the same solution. After stirring for 30 min at room temperature the mixture was analyzed by $^{31}P\{^{1}H\}$-NMR (161 MHz, CD_2Cl_2): 31.36 ppm (s), 23.46 ppm (s), 21.19 ppm (d, J_{P-P} = 20 Hz, J_{Pt-P} nd), 16.80 ppm (s, J_{Pt-P} = 3690 Hz, **10F′**), 11.54 ppm (s, J_{Pt-P} = 3282 Hz, **12F′**), 4.66 ppm (d, J_{P-P} = 20 Hz, J_{Pt-P} nd).

Rhodium(I) catalyzed hydroformylation of 1-octene

All the catalytic experiments herein presented were carried out in a parallel mode in a multi autoclave reactor AMTEC-SPR-16 from Advanced Machinery & Technology Chemnitz GmbH. The general procedure reads as follows: the autoclaves were purged twice with nitrogen at room temperature, two more times at 100 °C, and cooled to room temperature again. To each vessel were added: 3 mL of a Rh(I) stock solution (2.68 mM of Rh(acetylacetonate)$(CO)_2$) and 3 mL of a ligand stock solution/suspension (26.6 mM of monophosphine or 13.3 mM of diphosphine, and 13.3 mM of template, if required). The autoclaves were then pressurized with 20 bar of syngas and heated to 80 °C, stirring at 1000 rpm, for 90 min. After cooling to room temperature and depressurizing the vessels, 2 mL of a substrate stock solution (2.7 M of substrate and 15 mM of *n*-decane) were added. The autoclaves were then pressurized to 20 bar of syngas and heated to the reaction temperature, stirring at 1000 rpm, for 8 h approximately. Gas consumption was automatically monitored and data used to calculate conversions and turnover frequencies. Aliquots of 0.1 mL were taken automatically at 0.5, 1, 2, 4, and 8 h approx., quenched with triethyl phosphite, diluted with dichloromethane, and analyzed by GC-FID to determine final products and selectivity (supporting information†).

Table 5 Crystal data and structure refinement

Complex	**7C**	**9E′**
Formula	$C_{70}H_{76}C_{18}N_6O_{10}P_2Zn_2$	$C_{66}H_{70}N_4O_{10}P_2Zn_2$
Mr (g mol^{-1})	1637.65	1271.94
Crystal system	Monoclinic	Monoclinic
Space group	$P2_1/c$	$P2_1/n$
a/Å	8.8886(14)	18.8474(12)
b/Å	21.225(4)	7.8500(5)
c/Å	19.390(3)	20.6464(13)
α (°)	90.00	90.00
β (°)	90.878(8)	98.266(3)
γ (°)	90.00	90.00
V/Å^3	3657.7(10)	3022.9(3)
Z	2	2
D_c (g cm^{-1})	1.487	1.397
μ_{Mo} (mm^{-1})	1.053	0.909
T/K	100(2)	100(2)
F(000)	1688	1328
No. of reflns collected	6814	12184
No. of ind. reflns	2641	9971
R_{int}	0.2768	0.0454
Data/restraints/parameters	2641/54/482	9971/559/724
Goodness of fit on F^2	0.933	1.156
R_1 [$I > 2\sigma(I)$]	0.0915	0.0646
wR_2 [$I > 2\sigma(I)$]	0.1844	0.1687
R_1 (all data)	0.2536	0.0788
wR_2 (all data)	0.2497	0.1758
$2\theta_{max}$	51.28	67.92
Index ranges	$-9 \le h \le 10$ $-25 \le k \le 25$ $-19 \le l \le 23$	$-29 \le h \le 29$ $-8 \le k \le 12$ $-32 \le l \le 32$
Largest diff peak and hole/e Å^{-3}	1.537 and –0.907	2.782 and –0.777
Crystal size/mm	$0.05 \times 0.02 \times 0.005$	$0.20 \times 0.05 \times 0.02$

X-Ray crystallography

All crystals were mounted on a magnetic support with 10 micron nylon fiber cryoloop. Data were collected on a Bruker-Nonius diffractometer equipped with an APEX II 4 K CCD area detector, a FR591 rotating anode with Mo-Kα-radiation, MultiLayer Montel 200 Mirrors and a Kryoflex low temperature device (T = –173 °C). Full sphere data collection was carried out with ω and φ scans using Bruker APEX software (versions v1.0-22, v2009.1-0 and v2009.1-02, 2007, Bruker AXS Inc., Madison, Wisconsin, USA). Empirical absorption corrections were applied using SADABS (Version 2008/1 Bruker-Nonius.). Structures were solved by either Patterson or Direct Methods using SHELXS-97

and refined with SHELXL software (versions V6.12 and 6.14) (Table 5).

Acknowledgements

We thank the Ministerio de Ciéncia e Innovación of Spain for the financial support (CTQ2005-03416; BES-2006-11627), the members of the Research Support Unit of the ICIQ, Prof. Pau Ballester and his co-workers for their collaboration.

References

1 B. Breit and W. Seiche, *J. Am. Chem. Soc.*, 2003, **125**, 6608–6609.
2 Z. Freixa and P. W. N. M. van Leeuwen, *Dalton Trans.*, 2003, 1890–1901.
3 M. Dieguez, A. Ruiz and C. Claver, *J. Org. Chem.*, 2002, **67**, 3796–3801.
4 G. Rousseau and B. Breit, *Angew. Chem., Int. Ed.*, 2011, **50**, 2450–2494.
5 J. Meeuwissen and J. N. H. Reek, *Nat. Chem.*, 2010, **2**, 615–621.
6 *Supramolecular Catalysis*, ed. P. W. N. M. van Leeuwen, Wiley-VCH, Weinheim, 2008.
7 H. Gulyas, J. Benet-Buchholz, E. C. Escudero-Adan, Z. Freixa and P. W. N. M. van Leeuwen, *Chem.–Eur. J.*, 2007, **13**, 3424–3430.
8 D. Rivillo, H. Gulyas, J. Benet-Buchholz, C. Escudero-Adan Eduardo, Z. Freixa and P. W. N. M. van Leeuwen, *Angew. Chem., Int. Ed.*, 2007, **46**, 7247–7250.
9 J. M. Takacs, D. S. Reddy, S. A. Moteki, D. Wu and H. Palencia, *J. Am. Chem. Soc.*, 2004, **126**, 4494–4495.
10 J. N. H. Reek, M. Roeder, P. E. Goudriaan, P. C. J. Kamer, P. W. N. M. van Leeuwen and V. F. Slagt, *J. Organomet. Chem.*, 2005, **690**, 4505–4516.
11 V. F. Slagt, P. W. N. M. van Leeuwen and J. N. H. Reek, *Chem. Commun.*, 2003, 2474–2475.
12 M. Kuil, P. E. Goudriaan, P. W. N. M. van Leeuwen and J. N. H. Reek, *Chem. Commun.*, 2006, 4679–4681.
13 P. Guerriero, S. Tamburini and P. A. Vigato, *Coord. Chem. Rev.*, 1995, **139**, 17–243.
14 P. Guerriero, P. A. Vigato, D. E. Fenton and P. C. Hellier, *Acta Chem. Scand.*, 1992, **46**, 1025–1046.
15 P. A. Vigato and S. Tamburini, *Coord. Chem. Rev.*, 2004, **248**, 1717–2128.
16 P. A. Vigato, S. Tamburini and L. Bertolo, *Coord. Chem. Rev.*, 2007, **251**, 1311–1492.
17 W. Zhang, J. L. Loebach, S. R. Wilson and E. N. Jacobsen, *J. Am. Chem. Soc.*, 1990, **112**, 2801–2803.
18 T. Katsuki, *J. Mol. Catal. A: Chem.*, 1996, **113**, 87–107.
19 R. Robson, *Aust. J. Chem.*, 1970, **23**, 2217–2224.
20 W. Huang, S. Gou, D. Hu, S. Chantrapromma, H.-K. Fun and Q. Meng, *Inorg. Chem.*, 2002, **41**, 864–868.
21 A. W. Kleij, M. Kuil, D. M. Tooke, M. Lutz, A. L. Spek and J. N. H. Reek, *Chem.–Eur. J.*, 2005, **11**, 4743–4750.
22 J. Gao, J. H. Reibenspies and A. E. Martell, *Angew. Chem., Int. Ed.*, 2003, **42**, 6008–6012.
23 J. Gao, J. H. Reibenspies, R. A. Zingaro, F. R. Woolley, A. E. Martell and A. Clearfield, *Inorg. Chem.*, 2005, **44**, 232–241.
24 J. Gao, F. R. Woolley and R. A. Zingaro, *Org. Biomol. Chem.*, 2005, **3**, 2126–2128.
25 M. Kuil, P. E. Goudriaan, A. W. Kleij, D. M. Tooke, A. L. Spek, P. W. N. M. van Leeuwen and J. N. H. Reek, *Dalton Trans.*, 2007, 2311–2320.
26 T. Mizutani, K. Wada and S. Kitagawa, *J. Org. Chem.*, 2000, **65**, 6097–6106.
27 P. Ballester, A. Costa, A. M. Castilla, P. M. Deya, A. Frontera, R. M. Gomila and C. A. Hunter, *Chem.–Eur. J.*, 2005, **11**, 2196–2206.
28 A. W. Kleij, *Chem.–Eur. J.*, 2008, **14**, 10520–10529.
29 V. F. Slagt, J. N. H. Reek, P. C. J. Kamer and P. W. N. M. van Leeuwen, *Angew. Chem., Int. Ed.*, 2001, **40**, 4271–4274.
30 V. F. Slagt, P. C. J. Kamer, P. W. N. M. van Leeuwen and J. N. H. Reek, *J. Am. Chem. Soc.*, 2004, **126**, 1526–1536.
31 W. Huang, H. B. Zhu and S. H. Gou, *Coord. Chem. Rev.*, 2006, **250**, 414–423.
32 G. Machado, J. D. Scholten, T. de Vargas, S. R. Teixeira, L. H. Ronchi and J. Dupont, *Int. J. Nanotechnol.*, 2007, **4**, 541–563.
33 S. Mohanta, B. Adhikary, S. Baitalik and K. Nag, *New J. Chem.*, 2001, **25**, 1466–1471.
34 A. J. Atkins, D. Black, R. L. Finn, A. Marin-Becerra, A. J. Blake, L. Ruiz-Ramirez, W.-S. Li and M. Schroeder, *Dalton Trans.*, 2003, 1730–1737.
35 N. H. Pilkington and R. Robson, *Aust. J. Chem.*, 1970, **23**, 2225–2236.
36 L. F. Lindoy, G. V. Meehan and N. Svenstrup, *Synthesis*, 1998, 1029–1032.
37 S. R. Korupoju, N. Mangayarkarasi, S. Ameerunisha, E. J. Valente and P. S. Zacharias, *J. Chem. Soc., Dalton Trans.*, 2000, (16), 2845–2852.
38 J. Gao, Y. G. Liu, Y. Q. Zhou, L. M. Boxer, F. R. Woolley and R. A. Zingaro, *ChemBioChem*, 2007, **8**, 332–340.
39 B. Liu, H. Zhou, Z. Q. Pan, H. P. Zhang, J. D. Hu, X. L. Hu, H. Zhou and Y. Song, *Transition Met. Chem.*, 2005, **30**, 1020–1026.
40 W. Huang, S. Gou, D. Hu, S. Chantrapromma, H.-K. Fun and Q. Meng, *Inorg. Chem.*, 2001, **40**, 1712–1715.
41 B. Dutta, P. Bag, U. Floerke and K. Nag, *Inorg. Chem.*, 2005, **44**, 147–157.
42 W. Huang, Z. L. Chu, S. H. Gou and T. Ogawa, *Polyhedron*, 2007, **26**, 1483–1492.
43 W. Huang, D. Hu, S. Gou, S. Chantrapromma, H.-K. Fun, Y. Xu and Q. Meng, *Inorg. Chim. Acta*, 2003, **342**, 9–15.
44 W. Huang, S. Gou, H. Qian, D. Hu, S. Chantrapromma, H.-K. Fun and Q. Meng, *Eur. J. Inorg. Chem.*, 2003, 947–954.
45 Z. L. Chu and W. Huang, *Acta Crystallogr., Sect. E: Struct. Rep. Online*, 2006, **63**, m198–M200.
46 J. L. Fang, W. Huang, S. Chantrapromma, S. Shanmuga, Sundara Raj, I. A. Razak, H. K. Fun, S. H. Gou and H. S. Wang, *Acta Crystallogr., Sect. C: Cryst. Struct. Commun.*, 2000, **56**, 1429–1430.
47 W. Huang, S. H. Gou, D. H. Hu, Y. Xu, S. Chantrapromma and Q. J. Meng, *J. Mol. Struct.*, 2001, **561**, 121–129.
48 H. Adams, N. A. Bailey, P. Bertrand, C. O. Rodriguez de Barbarin, D. E. Fenton and S. Gou, *J. Chem. Soc., Dalton Trans.*, 1995, 275–279.
49 R. Rodriguez-Cortinas, F. Avecilla, C. Platas-Iglesias, D. Imbert, J. C. G. Bunzli, A. de Blas and T. Rodriguez-Blas, *Inorg. Chem.*, 2002, **41**, 5336–5349.
50 J.-L. Bai, H. Zhou, Z.-Q. Pan, R. Chen, J.-D. Hu, L. Wang and Y.-Z. Li, *Wuji Huaxue Xuebao*, 2008, **24**, 1994–2001.
51 M. A. Weiner and P. Schwartz, *Inorg. Chem.*, 1975, **14**, 1714–1716.
52 O. Herd, A. Hessler, M. Hingst, M. Tepper and O. Stelzer, *J. Organomet. Chem.*, 1996, **522**, 69–76.
53 I. M. Al-Najjar, *Inorg. Chim. Acta*, 1987, **128**, 93–104.
54 G. P. C. M. Dekker, C. J. Elsevier, K. Vrieze, P. W. N. M. van Leeuwen and C. F. Roobeek, *J. Organomet. Chem.*, 1992, **430**, 357–372.
55 E. Lindner, R. Fawzi, H. A. Mayer, K. Eichele and W. Hiller, *Organometallics*, 1992, **11**, 1033–1043.
56 M. Kranenburg, Y. E. M. van der Burgt, P. C. J. Kamer, P. W. N. M. van Leeuwen, K. Goubitz and J. Fraanje, *Organometallics*, 1995, **14**, 3081–3089.
57 C. P. Casey and G. T. Whiteker, *Isr. J. Chem.*, 1990, **30**, 299–304.
58 L. A. van der Veen, P. H. Keeven, G. C. Schoemaker, J. N. H. Reek, P. C. J. Kamer, P. W. N. M. van Leeuwen, M. Lutz and A. L. Spek, *Organometallics*, 2000, **19**, 872–883.
59 A. Buhling, P. C. J. Kamer and P. W. N. M. van Leeuwen, *J. Mol. Catal. A: Chem.*, 1995, **98**, 69–80.
60 S. Mohanta, B. Adhikary, S. Baitalik and K. Nag, *New J. Chem.*, 2001, **25**, 1466–1471.
61 M. Nishimura, M. Ueda and N. Miyaura, *Tetrahedron*, 2002, **58**, 5779–5787.
62 D. T. Rosa, R. A. Reynolds III, S. M. Malinak, D. Coucouvanis, M. Ali and F. M. MacDonnell, *Inorg. Synth.*, 2002, **33**, 112–119.
63 F. Y. Kwong, C. W. Lai, M. Yu and K. S. Chan, *Tetrahedron*, 2004, **60**, 5635–5645.